European Review for Medical and Pharmacological Sciences 2023; 27: 9375-9387

Tubermycin B coated on Galactosylated Chitosan Nanoparticles synthesized by eco-friendly method ameliorates intracellular free radical production and reduces oxidative stress, reducing phosphorylation of IKKα/β/plκBα/NF-κB pathway

A.S. BINSHAYA[1], S.A. ALGHAMDI[1], N.S. ALHARTHI[1], A. HJAZI[1], A.A. ALQASEM[1], H.H. ALMASOUDI[2], F.M. ALDAKHEEL[3], D. FALLATAH[1], N.E. ALMOAMMAR[1], G.S. ALORAINI[1], M.S. ALOAHD[4]

[1]Department of Medical Laboratory Sciences, College of Applied Medical Sciences, Prince Sattam bin Abdulaziz University, Alkharj, Saudi Arabia.
[2]Department of Clinical Laboratory Sciences, College of Applied Medical Sciences, Najran University, Najran, Saudi Arabia
[3]Department of Clinical Laboratory Sciences, College of Applied Medical Sciences, King Saud University, Riyadh, Saudi Arabia
[4]College of Life Science, Maulana Azad College of Arts and Science, Aurangabad, India

Abstract. – OBJECTIVE: The objective of the current study was to investigate the cytotoxic potentials of Galactosylated Chitosan Nanoparticles. Specifically, the study aimed to develop Tubermycin B coated on Galactosylated Chitosan Nanoparticles using a new green method that replaces sodium borohydride in the reduction process.

MATERIALS AND METHODS: The study synthesized Tubermycin B coated on Galactosylated Chitosan Nanoparticles through a new green method. The cytotoxicity of these nanoparticles was evaluated in a mice intestinal tract model that had been induced with chlorpyrifos, which causes oxidative stress-related enterotoxicity. Multiple activities, including the apoptosis of intestinal macrophages and the activation of Ikappa α/β kinase (IKKα/β), were examined as indicators of the nanoparticles' efficacy. The stability of the synthesized Chitosan Nanoparticles was also assessed. Additionally, the encapsulation efficiency of *Boscia angustifalia* and *Boscia senegalensis* extracts within the nanoparticles was determined.

RESULTS: The results of the study showed that Tubermycin B coated on Galactosylated Chitosan Nanoparticles effectively alleviated the oxidative stress-related enterotoxicity in the mice intestinal tract induced by chlorpyrifos. The nanoparticles prevented the apoptosis of intestinal macrophages and inhibited the activation of IKKα/β. The synthesized chitosan nanoparticles exhibited high stability. The encapsulation efficiency of *Boscia angustifalia* extract was recorded as 46.58%, whereas for *Boscia senegalensis* extract, it was 9.77%. The nanoparticles showed no cytotoxicity at all tested concentrations and demonstrated a medium-level anticancer effect.

CONCLUSIONS: Based on the findings, it can be concluded that Tubermycin B coated on Galactosylated Chitosan Nanoparticles has the potential to alleviate oxidative stress-related enterotoxicity in the mice intestinal tract. The nanoparticles showed high stability and exhibited a medium-level anticancer effect. Furthermore, the study demonstrated that *Boscia angustifalia* extract exhibited higher anti-hepatitis C virus antibodies (anti-HCV) activity compared to *Boscia senegalensis* extract in an *in-vitro* system. Therefore, *Boscia angustifalia* could be considered a promising candidate for the development of an anti-HCV drug for future *in-vivo* studies.

Key Words:
Tubermycin B, Galactosylated Chitosan, Nanoparticles, Intracellular free radical production, Oxidative stress.

Corresponding Authors: Mustafa Sawsan Aloahd, MD, Ph.D; e-mail: malmutairik@gmail.com
Abdulkarim S. Binshaya, MD, SA; e-mail: abd.aldosari@psau.edu.sa

Introduction

The increasing application of nanoparticles (NPs) in medical diagnostics and therapeutics has led to a growing interest in nanotoxicology and understanding the potentially toxic effects of NPs on the human body[1-3]. NPs, due to their small size, can easily penetrate biological barriers and reach various organs, causing toxic reactions[4,5]. Therefore, it is crucial to study the nanotoxicology of these materials and evaluate their mechanisms of toxicity before their application in domains such as pharmaceuticals, food, health, and diagnostics to prevent any negative impacts[6-10].

Cell viability assessment is commonly performed using tetrazolium-based assays, while the ELISA procedure is used to determine the inflammatory biomarkers triggered by NPs. Peripheral Blood Mononuclear Cells (PBMC) are composed mainly of T-cells and are suitable for investigating the immunological response in humans[11-13]. When reactive oxygen species (ROS) are produced excessively, oxidative stress occurs, leading to cellular damage. Balancing ROS levels through the antioxidant system is crucial for maintaining cellular homeostasis. Chitosan, derived from chitin, possesses unique properties such as biocompatibility, low toxicity, and biodegradability, making it an ideal material for drug delivery and tissue engineering applications. By modifying Chitosan with Galactose, it can be used as a targeted drug delivery agent for liver disorders[14-16].

Previous studies[15,16] have explored the synthesis of Galactosylated Chitosan using different methods. Chitosan is less abundant in living organisms compared to chitin, but certain fungal species contain Chitosan in their cell walls. Chitosan has various applications in the food industry, water purification, and biochemical processes. *Brevibacterium sp*. has shown potential as a pharmaceutical component for cancer treatment. The current study aims to investigate the behavior of NPs in an *in vitro* setting, specifically their interaction with the biological system. It focuses on the cytotoxic potential of the NPs using PBMC cells and examines their impact on intracellular free radicals and oxidative stress[15-17]. The study also involves a new green method for reducing chitosan using 6-(1-Hydroxyethyl) phenazine-1-carboxylic acid and ascorbic acid, replacing sodium borohydride, and encapsulating 6-(1-Hydroxyethyl) phenazine-1-carboxylic acid. This study aims to enhance our understanding of how NPs interact with the biological system through an *in-vitro* analysis. It investigates the cytotoxic potential of the NPs using PBMC cells and evaluates their impact on intracellular free radicals and oxidative stress. The study also presents a new green method for synthesizing Galactosylated Chitosan Nanoparticles.

Materials and Methods

Extraction and Purification of Chitosan

In line with the protocol developed earlier by Miler[17,18], (1959), the extraction of the Chitosan was performed. The activity of the chitosanase was validated by determining the reducing sugars, created by chitosan. With the help of the dinitrosalicylic acid method (Miller 1959)[17], the reducing sugars in the supernatant were determined, and glucosamine was used as a calibration standard. A unit of chitosanase is calculated as the volume of an enzyme that liberated 1 µmol D-glucosamine/minute as per the standards mentioned earlier. The MS-chitosan broth was used to cultivate the selected isolates of *A.flavus* at a temperature of 30°C for about 48 hours at 180 rpm in a rotary shaker. Then, the culture broth was centrifuged at 6,000 x for about 10 minutes. The supernatant was collected and subjected to fractionation using ammonium sulfate (Saudi Chemical Holding Company, Al-Malaz, Riyadh, Saudi Arabia) at varying saturation ratios i.e., 20-70%. Then, the sample was allowed to settle overnight at 4°C, after which it was centrifuged at 6,000 rpm for about 15 minutes. The precipitate was collected, and 30 mM phosphate buffer (pH 6.5) was added to dissolve the precipitate. Then, the solution was dialyzed overnight using the same buffer. The resultant solution was then stored in dialysis tubes.

The dialysis tubes were treated with Polyethylene glycol (PEG) (Saudi Chemical Holding Company, Al-Malaz, Riyadh, Saudi Arabia) powder by scattering them around the tubes. Thus, the PEG-treated dialysis tubes were kept under incubation at 4°C until the size of the tubes shrunk to 2/10 of their actual volume. The PEG-concentrated enzyme solution was made to undergo dialysis against phosphate buffer (30 mM; pH 6.5). Then, the solution was run in the Diethylaminoethyl cellulose (DEAE) cellulose column (2x25 cm) that was equilibrated with the same buffer. Using the equilibration buffer, the column was washed, after that, the elution of the chitosanase was performed with 0 to 0.5 M NaCl. After the concentration of the chitosanase fractions, it was subjected to gel permeation chromatography with the help of a Sephadex G-100 column (2x80 cm). The column

was already equilibrated using phosphate buffer (10 mM; pH 6.5) while it was again used for elution. The active fractions were then collected to conduct an additional investigation. Fourier-transform infrared spectroscopy (FT-IR) (Thermo Nicolet Model- Avatar 320 model, Vista, CA, USA) was used to evaluate the Chitosan, extracted from the cell walls of *A.flavus*. Then, the sample's peak values were contrasted against the standard Chitosan, isolated from the shells of crabs.

6-(1-Hydroxyethyl) Phenazine-1-Carboxylic Acid (HPCA) Extraction and Purification from Brevibactrium sps

The Zobell broth was used for the cultivation of HPCA from *Brevibactrium sps* isolate. After the inoculation, the broth was kept under incubation in favorable conditions to obtain the highest possible activity. Then, the *Brevibactrium* culture's crude extract was nurtured under certain favorable conditions and was allowed to run through preparative High-performance liquid chromatography (HPLC) (Thermo Nicolet Model-Avatar 320 model, Vista, CA, USA) with the help of gradient elution containing 10-90% aqueous acetonitrile for 1 h (flow rate 0.8 ml/min) and it yielded 15 fractions. As detailed earlier, every fraction was analyzed for its cytotoxic activity. After a significant activity was found in Fraction VIII, it was again fractionated using reversed-phase HPLC, in which a gradient elution of 30-100% aqueous methanol was used for about 1 h (flow rate 5 ml/min) to obtain a major subfraction (fraction VIII-1) and two minor subfractions (VIII 2 and 3). Under the electron ionization mode, the mass spectrum of every fraction was analyzed by scanning the samples at 40 to 600 *m/z*. The Gas-liquid Chromatography Mass Spectrometer [GC-MS, (Thermo Nicolet Model-Avater, Vista, CA, USA)] peaks of unknown compounds were identified by the researchers through a comparison of the spectra, their profiles and similarity levels against the standard values set by the National Institute of Standard and Technology (2005, USA) and the Wiley 275 libraries.

Galactosylated Nanochitosan Preparation

The ionotropic gelation method was followed to prepare the Chitosan Nanoparticles, in which the Chitosan was allowed to interact with sodium polyphosphate anions. The Chitosan's amino groups contain positive charges, which were cross-linked with those of the negative charges present in sodium polyphosphate. Wang et al[7] method was followed to prepare the Galactosylated Nanochitosan in which a major modification was introduced i.e., the replacement of sodium borohydride with L-ascorbic acid, which is not only eco-sensitive but also biocompatible. To be precise, the Chitosan (0.075 g) and distilled water (50 ml) were mixed with acetic acid (0.5 ml). On the other hand, the sodium polyphosphate (0.03 g) was dissolved in 25 ml of distilled water, and the solution was added to the Chitosan solution in a dropwise fashion. This eventually led to the production of clear Chitosan NPs that are now termed Cs. The researchers added 1.6 gm of ascorbic acid to the NPs prepared earlier, to reduce the Nanochitosan particles. The solution was placed in a stirrer for up to one hour, which was termed as (Cs + As). After this process, 8 g of lactose was added in (Cs + As) and stirred for an hour, and the solution is termed now as Cs + As + Lact. Then, the centrifugation of the NPs was performed, after which it was washed using distilled water three times to get rid of the unreacted ascorbic acid and lactose. Afterward, it was freeze-dried for about 48 hours.

Preparation of HPCA Loaded Nano Galactosylated Chitosan

The preparation of the HPCA-loaded Nanochitosan was accomplished by dissolving three varying concentrations of the extracts, from each species in the range of (100, 200, and 300 µg) in 25 ml of distilled water. Afterward, sodium polyphosphate (NaPp) was added to the solution, as discussed earlier. Then, the solution was mixed with the Chitosan solution in a dropwise fashion. In line with the method followed earlier, the galactosylation of the nanoparticles was performed.

Characterizations of HPCA Loaded Nano Galactosylated Chitosan (HNGC)

To analyze the morphological characteristics of the nanoparticles prepared in this study and their characterization, the field emission Scanning Electron Microscope SEM (Jeol JXA 840, Electron Microscope, TEM-HR, Quito, Japan) was used. Fourier Transform Infrared (FT-IR) spectrophotometer (model FT/IR-6,100 type A, Jasco, Minzen, Germany) was used to validate whether the NP size got reduced and galactosylated. Further, its effect on drug addiction was also analyzed through this model. In addition to the above, Transmission electron microscopy (TEM) (JEOL, JEM2100, Electron Microscope, TEM-HR, Quito, Japan) was utilized to investigate the shape

and size of the NPs prepared for the study. To measure the zeta potential, Polydispersity Index (PDI), and the size of the particles, Zeta sizer and Zeta potential measurements (Malvern 107,474) were utilized.

Encapsulation Efficiency

The authors analyzed the efficiency of the encapsulation process through a comparison of the differences in absorbance rate of the extract (the primary concentration) and free drug (the unencapsulated) as per the literature[19].

In Vitro Cell Culture

The authors procured the RAW264.7 cells and Human B-cell lymphoma cells DOHH2 from BeNa Culture Collection. RAW264.7, derived from murine macrophages, is used as a model system to study immunological and pharmacological research. They are adherent cells that can be cultured *in vitro* and are easy to maintain. DOHH2 is a human B-cell lymphoma cell line derived from a patient with follicular lymphoma. These cells are widely used in research related to lymphoma and B-cell biology. They express various B-cell markers and exhibit typical features of B-cell lymphomas. DOHH2 cells have been employed as a model system to investigate the molecular mechanisms underlying drug sensitivity, and potential therapeutic interventions.

Top of Form

These procured cells were cultured in Dulbecco's Modified Eagle Medium (DMEM) medium, which contains a balanced mixture of amino acids, glucose, vitamins, and salts, supplemented with fetal bovine serum (FBS) and antibiotics for optimal cell growth and viability. Penicillin/streptomycin was used at a final concentration of 100 units/mL of penicillin and 100 µg/mL of streptomycin. Amphotericin B is added at a concentration of 0.25-0.5 µg/mL. In addition to these, the culture was also added with heat-inactivated FBS to 10% final concentration. Subsequent experiments were conducted using these culture cells until the cells and the confluence were maintained. For the experiments, the cells at the exponential growth phase were used. After 2-3 times of passage, the procured cells were utilized.

In Vivo Animal Experiments and Design

For this study, the researchers procured animals from Changchun Yisi Laboratory Animal Co., LTD. The male mice, C57BL/6J aged 8 weeks and weighing 20-22 g, were used for the study (Certificate number 2021/0726/001, Changchun, China). For 7 days, the mice were housed under a 12-hour light-dark cycle to acclimate to the environment. The environmental conditions maintained were as follows: temperature 22°C and 10% relative humidity. During the 12/12-hour light-dark cycle, the mice were given free access to food and drinking water. In line with the guidelines framed by Animal Care and Use Guidelines, the animals were taken care of. The Experimental Animal Ethics Committee guidelines were adhered to when conducting the experimental procedures. Each group in the study contained 8 animals.

Treatment Protocol

For the animals, the authors administered the HNGC (5 mg/kg), which was dissolved in 0.1% dimethyl sulfoxide (DMSO) (Sigma Chemical Company, California, CA, USA). Every day, the nanocomposite (0.1 ml/10g body weight) was administered orally to the mice for about three weeks. On the other hand, the DMSO (0.1%) was provided to the control group animals. The current study made use of the highest effective dose as per the suggestion from studies[13,14]. There was no change in the OS indices' level in the groups administered with nanoparticle and composite, at the same concentration.

Biological Evaluation of Encapsulated Drugs

Cytotoxicity testing

To analyze the activities of NPs, the cytotoxicity against RAW264.7 and DOHH2 was validated to determine the IC_{50}. The inoculation of the DOHH2 cells was performed at a rate of $1x10^4$ cells/100 µl medium/well in a 96-well plate. After a day i.e., 24 hours, the media was aspirated, after which the samples were made to undergo serial dilution (tested concentrations equivalent to *Boscia* extract: 12.5, 25, and 50 µg/ml) in Roswell Park Memorial Institute (RPMI) medium (2% FBS) and the culture was kept under incubation for 24 hrs. After the aspiration of the media containing samples, from each well, 20 µl of 0.5% crystal violet solution was added. Then, the solution was kept under incubation at room temperature for about 10 minutes. Then, the solution was washed thrice using 200 µl of distilled water. Every well was then added with 200 microliters of methanol and the incubation of the plate was performed for 20 minutes at room temperature. Then, the absorbance level was determined at 570 nm in an

Enzyme-linked immunosorbent assay (ELISA) reader. Then, the following equation was used to determine the efficiency of every sample.

% cell viability = (absorbance of extracts treated cells/absorbance of control cells) × 100

All the experiments were conducted thrice, whereas the mean values were considered for calculations.

ROS detection

The authors determined the intracellular ROS levels with the help of the fluorescent probe 2',7'-Dichlorofluorescin diacetate (DCFH-DA). Six-well culture plates were inoculated with $1x10^5$ RAW264.7 cells/well and was kept undisturbed for about 12 hours in a complete RPMI medium. Then, the cells were washed using PBS twice and kept under incubation along with 10 μM DCFH-DA at 37°C for 20 mins. Then, PBS was used to wash the cells thrice, after which the flow cytometry method was followed to determine the fluorescence intensity of intracellular ROS.

Western Blotting for Expression Analysis of Apoptosis-Related Proteins

In this analysis, the cell lines were utilized for expression analysis, while the DMSO-treated cells were utilized as control. In this experiment, the $1x10^5$ RAW264.7 cells/well were inoculated in 6-well plates, while every well was populated with 10^7 cells and kept under incubation for adherence. Then, the cells were supplemented with UQAIR-11 fraction VIII-1 (HPCA) for treatment at different concentrations, including IC_{50}. Afterward, RAW264.7 cells were stimulated using Lipopolysacchride (1 μg/mL) and kept under incubation for about 36 h. Ice-cold Radioimmunoprecipitation buffer with a proteinase cocktail was used to lyse the Trypsinized cells. From the wells, the supernatants were collected and made to undergo protein normalization. Then, it was utilized to conduct the western blot experiments. From every sample, about 100 μg protein was made to undergo 12% sodium dodecyl sulfate-polyacrylamide gel electrophoresis (SDS PAGE), after which it was shifted to nitrocellulose, blocked using 10% nonfat milk at 4°C overnight. The incubation of the blotted membrane was performed under different antibodies like NF-κB (Nuclear factor light chain kappa activator of B cell), IκBα (anti-inhibitor of NF-κB alpha), phosphorylated-IκBα, p65 (a subunit of NF-kappa-B transcription complex), anti-extracellular signal-regulated kinase 1/2 (ERK1/2), anti-phospho-ERK1/2, anti- c-Jun N-terminal kinase (JNK), anti-phospho-JNK, anti-p38, antiphospho-p38, caspase-3 cleaved (cysteine-dependent aspartate-directed proteases), PARP cleaved (Poly ADP ribose polymerase) and β-actin (internal control) primary antibodies (Cell signaling, CST, CA, USA). Afterward, the detection of the primary antibodies was performed with the help of horseradish peroxidase-conjugated anti-rabbit secondary antibody (Cell signaling, CST, CA, USA) and the improved chemiluminescence reagents (BioRad, Banglore, India). In this study, ChemiDoc Imaging Systems (BioRad, Banglore, India) was utilized for the visualization of the bands.

Analysis of Blood Parameters

The complete set of assays was conducted after 24 hours of treatment. Once the designated period was completed, the mice's blood samples were collected by the researchers using capillary tubes. The number of red blood cells (RBCs), total white blood cells (WBCs), packed cell volume, hemoglobin content, and blood platelets were determined using the automated parameter hematology analyzer (T 450, cell counter, CA, USA). As per the protocol, the erythrocyte lysates were made. Then, the solution was centrifuged to get rid of the cell membranes, after which the supernatant was collected. This was utilized in the determination of oxidative stress indices, discussed in later sections.

Biochemical Analysis

Analysis of serum oxidative stress index

After executing the mice at the designated time, the researchers excised their liver and kidneys and washed them using ice-cold normal saline, after which it was homogenized at ice-cold temperature. To analyze the activity levels of ROS, total antioxidant capacity (T-AOC), measuring malondialdehyde formation (Thiobarbituric Acid Reactive Substance; TBARS)[15] and mitigated levels of glutathione (GSH)[20], Glutathione S-transferase (GST)[21], Catalase (CAT) activity[22] and Superoxide dismutase (SOD)[23] in mouse serum, the researchers used Bio-Rad ELISA reader and followed the instructions provided by the manufacturer. This experiment was conducted in line with the literature. The hemolysis samples were

not included as a part of this analysis, as per the instructions from the manufacturer.

Statistical Analysis

The groups were determined for their statistical significance and compared based on Analysis of variance (ANOVA), while the post-hoc testing was conducted based on Student-Newman-Keuls Multiple Comparison Tests. In this study, Statistical Package for the Social Sciences 19.0 (SPSS, Asia Analytics, Shanghai, China) was used to conduct the study analysis. The study data is expressed as mean ± standard deviation (mean ± sd), while the comparative analysis was conducted between the groups using the independent-samples *t*-test. To evaluate the diagnostic values, the Receiver operating characteristic (ROC) curve method was leveraged. Further, the correlation was analyzed using Pearson's correlation analysis. $p < 0.05$ denotes a significant difference.

Results

Extraction of Chitosan

In Yeast Extract, Peptone, Glycerol (YPG) medium, maximum growth of *Aspergillus flavus* was observed. This medium was recommended by Muslim et al[23] as the optimal one to synthesize Chitosan. Further, the production of Chitosan and the biomass production of *Aspergillus flavus* holds a relationship.

Characterization of Chitosan

The current study recorded a yield of 53.8% Chitosan, while its pH was 7.8. In general, Chitosan's purity can be understood from its solubility in acetic acid. The Chitosan's concentration in the acetic acid was 8.5 g/L, which denotes that the produced Chitosan was 85% pure (Figure 1a-b).

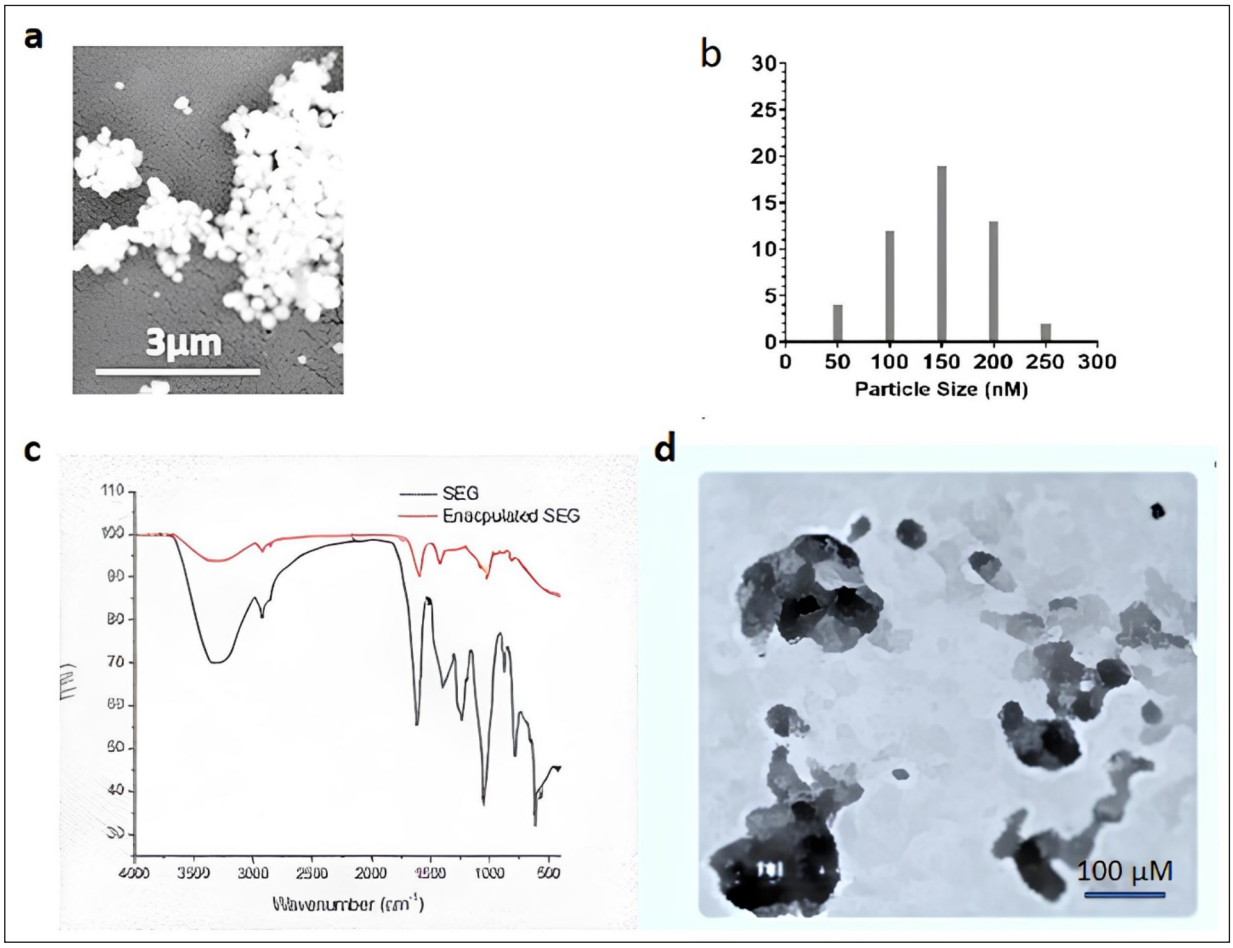

Figure 1. **a**, Showing of Characterization of Chitosan nanoparticles, **b**, The chitosan's concentration in the acetic acid was 8.5 g/L, which denotes that the produced chitosan was 85% pure, **c**, The purified chitosan achieved the same peaks as the peaks achieved by crab shell-derived standard chitosan, **d**, TEM was utilized to conduct a structural analysis of the Cs and GCs with two variants of drug extracts containing nanoparticles.

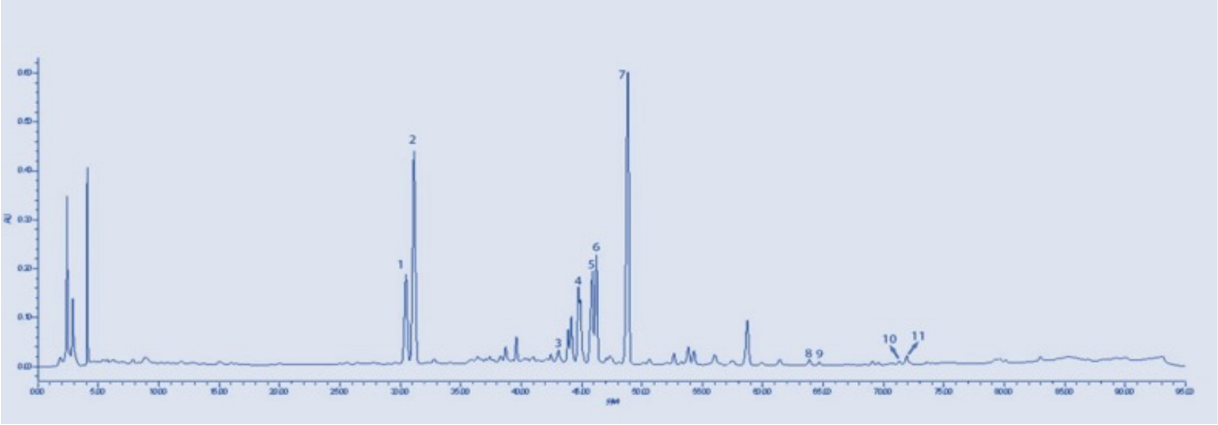

Figure 2. HPLC analysis. Out of the 15 major fractions exhibited during the preparative HPLC of HPCA, fraction VIII was found to be accountable for the expression of cytotoxic characteristics.

Characterization of Chitosan

The purified Chitosan achieved the same peaks as the peaks achieved by crab shell-derived standard Chitosan. In this study, two major peaks were obtained at ~3398.2 cm^{-1}, thus establishing the presence of a hydroxy group and ~1,645 cm^{-1}, assuring the existence of an amide band. The rest of the peaks, attained in this study, were ~2,367 cm^{-1}, ~2,233 cm^{-1}, and ~ 1,015 cm-^{1}. The peak was obtained at ~1,446 cm^{-1}, thus establishing the existence of the CH3 group, whereas the peak observed at ~1,515 cm^{-1} denotes the deformation of N-H in the amide group (Figure 1c-d, Figure 2).

Characterization of HPCA

Out of the 15 major fractions exhibited during the preparative HPLC of HPCA, fraction VIII was found to be accountable for the expression of cytotoxic characteristics. So, fraction VIII was then purified to narrow down the individual's efficacy. In the Gas Chromatography-Mass Spectrum (GC-MS) analysis, the authors found two minor and one major component of this fraction. About 83% of the total volume was contributed by the major component VIII-1 (HPCA), according to which the molecular formula was assigned i.e., C15H-12N2O3 by HR–EI–MS ((M)+¼ 268.272). As per the FTIR spectra, the highest possible absorption was found in line with the core phenazine structure and confirmed through comparison analysis with the HPLC-UV database. Holistic integration of the 2D Two-Dimensional Nuclear Magnetic Resonance (2D-NMR) data resulted in the development of a phenazine structure with a primary amide and a hydroxymethyl functionality. Such data is supported to dedicate the structure of the UQAIR-11 fraction VIII as 6-hydroxymethyl-1-phenazine-carboxamide (HPCA) (Figures 1-2).

Drug-loaded HPCA Loaded Nano Galactosylated Chitosan (HNGC) Spheres

Transmission electron microscopy

TEM was utilized to conduct a structural analysis of the Cs and GCs with two variants of drug extracts containing nanoparticles. The whole set of nanoparticles was spherical. Due to the encapsulation of the drug, there was a slight increase observed in the size, while the shape of the nanoparticles exhibited a slightly different morphology. In comparison with the *Boscia Seg*, the outer shell of *Boscia Aug*. was smaller. Further, the loaded drug was found to be bigger in the case of *Boscia Aug*. compared to *Boscia Seg*. This difference and the change in size between the loaded and the unloaded nanoparticles denote that both the drug extracts got encapsulated within the Chitosan matrix. The zeta sizer found that the size of different nanoparticles was almost the same (200 nm), for which the discussion is underway (Figure 1d) (Table I).

RBCs Toxicity Assay

As per the outcomes, it can be concluded that the samples remained safe, for the analyzed concentrations, since the hemolysis rate did not go above 8% at the maximum concentration. Figure 3 shows that the maximum hemolysis effect was observed at 50 µg/ml concentration, while the least hemolysis rate was 0.13 ± 0.07% for the tested concentration of 25 µg/ml. A high statistical significance (p = 0.004) was found among different samples at the same concentration level.

Table I. The zeta potential, size, and PDI of the prepared nanoparticles.

Sample	Zeta potential (mV)	Size (nm)	PDI
Chitsan	41.4 ± 0.59	199.5	0.579
HPCA	36.5 ± 2.34	213.5	0.621
HNGC	34.2 ± 2.34	224.7	0.7347

mV-millivolt, nm-Nanometer, PDI- Polydispersity Index.

Cytotoxicity on DOHH2 and RAW264.7 Cells

The concentration of all the samples did not reach the IC_{50} level as per the cytotoxicity of the samples on RAW264.7 cells and DOHH2 cells. These research findings infer that the samples exhibited minimal cytotoxicity at the highest evaluated concentrations (50 µg/ml), as portrayed in Figure 4. Therefore, the evaluated concentrations (12.5, 25, and 50 µg/ml) were found to be safe on DOHH2, when applied in anti-HCV activity assay. Two-way ANOVA was conducted, which found a significant decline in the cytotoxicity level for every sample by reducing the concentration ($p = 0.02$). These findings were in alignment with that of the literature on *B. senegalensis* methanolic extract, which found a medium-level antitumor activity of the extract on DOHH2 cells. The existence of a galactose moiety, in the prepared-loaded chitosan nanospheres, functions as a specific ligand to the asialoglycoprotein receptor (ASGP-R) found in the hepatocellular carcinoma cells, which in turn increases the cellular uptake of the NPs. When the galactose ligand binds with the ASGP-R, it promotes liver-targeted drug delivery. The study findings thus confirm that the prepared Chitosan NPs exhibit moderate anti-tumor activity against the DOHH2 cells (Figure 4).

Biochemical Analysis

HNGC can improve oxidative stress and enhance antioxidant activity

The thiobarbituric acid reactive substances (TBARS) in organs (such as the liver and kidneys) was found to be significantly decreased ($p < 0.005$) in mice administered with HNGC. A remarkable decline ($p < 0.001$) was observed in the TBARS lipid peroxidation, GSH, GST, CAT, and SOD levels in the hepatic (Figure 5A), renal cells (Figure 5B), and in red blood cells (Figure 5C), that were treated with HNGC. These changes were compared to the control and indicated that HNGC does not have any major effects on body tissues and their metabolism. As per the outcomes achieved from the serum and intestinal tissue's oxidative stress-related indices, it can be confirmed that TBARS lipid peroxidation, GSH, GST, CAT, and SOD in the control group were remarkably higher compared to the HNGC group. However, a significant decline was observed in the SOD level ($p < 0.05$, $p < 0.01$). The oxidative system got normal with HNGC, which infers that exposure to HNGC improves the mechanical barrier of the mouse (Figure 5).

HNGC Reduces Phosphorylation and Inflammatory Oxidative Stress of IKKα/β and plκBα in Intestinal Tissues

As per the outcomes, there was a relationship between the activation of IKK/IκBα/NF-κB pathway and chlorpyrifos (CPF)-induced enterotoxicity. Figure 6 shows a significant increase in the protein expression levels of p-IKKα/β and p-IκBα after exposure to CPF in comparison with the control group. Further, the CPF group exhibited significantly higher expressions of Cyt-c and

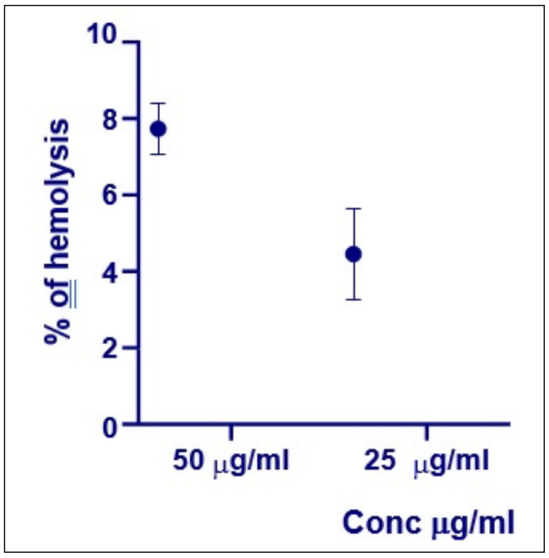

Figure 3. RBCs toxicity assay. Maximum hemolysis effect was observed at 50 µg/ml concentration, while the least hemolysis rate was 0.13 ± 0.07% for the tested concentration of 25 µg/ml.

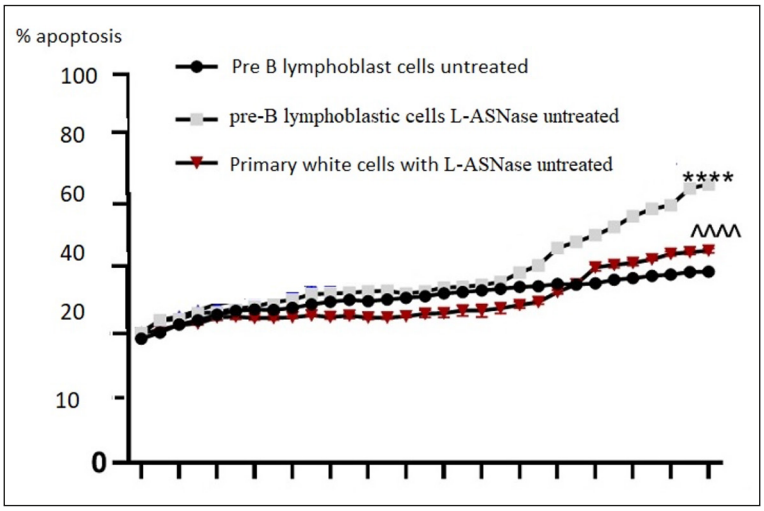

Figure 4. Apoptosis analysis. These research findings infer that the samples exhibited minimal cytotoxicity at the highest evaluated concentrations (50 µg/ml).

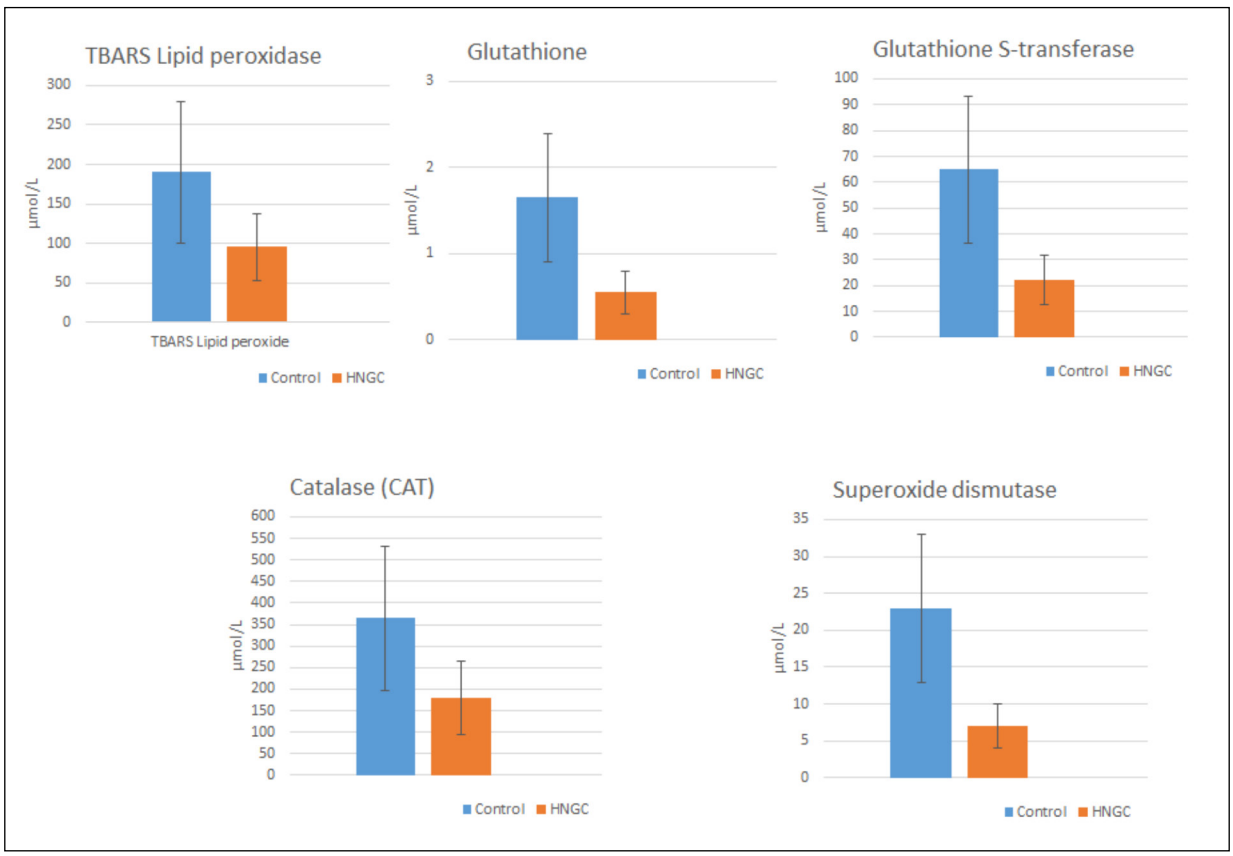

Figure 5. HNGC analysis of oxidative stress and enhanced antioxidant activity. These changes were compared to the control and indicate that HNGC does not have any major effects on body tissues and their metabolism.

Caspase-3 than the control group, thus inferring the occurrence of CPF-induced apoptosis. However, a decline was observed in the expressions of both groups in the GSLS-H group. The results infer that GSLS can effectively mitigate the apoptosis of pesticide-poisoning mice. Altogether, the data recommend that GSLS can effectively ameliorate enterotoxicity through efficient prevention

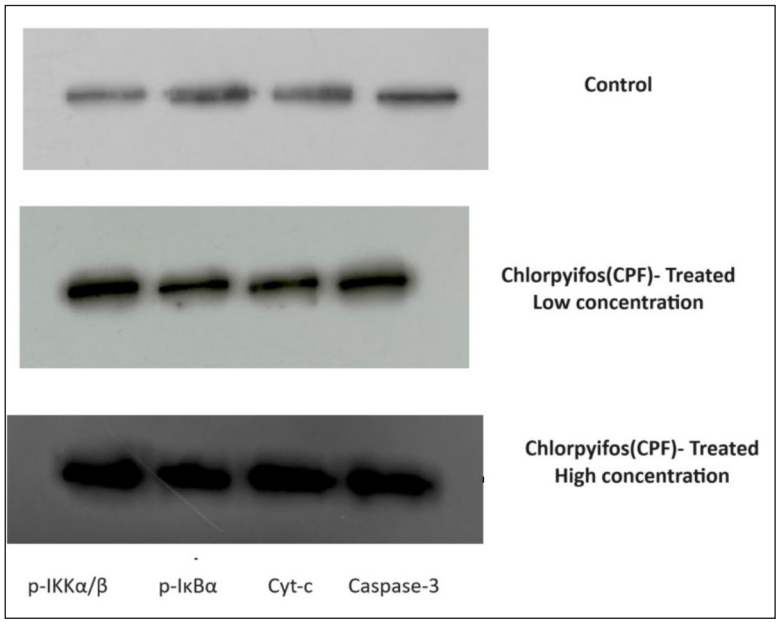

Figure 6. HNGC reduces phosphorylation and inflammatory oxidative stress of IKKα/β and pIκBα in intestinal tissues. A significant increase in the protein expression levels of p-IKKα/β and p-IκBα, Cyt-c and Caspase-3.

of the CPF-induced increase in IKKα/β and pIκBα phosphorylation in the mouse gut.

Discussion

In this study, the extraction of the Chitosan was performed with the help of demineralization and deproteinization. Chitosan production from endophytic fungi is one of the best alternative and cost-effective solutions instead of its traditional production from the shells of crustaceans. The fungi-produced Chitosan recovery process has been standardized and scaled up for industrial production already. In comparison with chitin, Chitosan possesses high volumes of highly protonated free amino groups that tend to attract the ionic compounds, as per the FTIR results[24]. This is the rationale behind the solubility of Chitosan in inorganic acids[25]. Various research[26,27] works have been conducted to evaluate and screen the natural antioxidants, across the globe. In this background, the current research work assessed the impact of curcumin as well as Chitosan on Cadmium toxicity. The results achieved from the study infer that the natural nanoparticles and nanocomposites have the potential to ameliorate the oxidative damage triggered by Cd-induced toxicity in the liver, kidneys, and red blood cells of mice. The study outcomes showcase that both Chitosan and curcumin NPs can act as excellent antioxidants and can overcome the disastrous impact created by oxidative stress.

Under pathological conditions, the ROS increases significantly in intestinal macrophages as a result of intestinal barrier dysfunction and enterotoxicity. When the human body is exposed to chlorpyrifos, it results in a heavy accumulation of ROS among RAW264.7 cells. This phenomenon prevents the intestinal cells from normal functioning. It is interesting to note that when treated with GSLS, all these adverse effects were reversed. Being an intracellular enzyme in the intestinal epithelium cells, diamine oxidase (DAO)'s activities tend to change, and this has a close connection with damage and repair of the intestinal mucosal epithelial cells[28]. So, the intestinal injury can be determined using an indicator i.e., the presence of DAO content in the mouse intestinal tissue. As per the current study results, there was a significant increase found in the DAO content in the intestinal tissues of CPF group mice. However, a remarkable decline was observed in the DAO content in the GSLS group (GSLS-L and GSLS-H). Similarly, the CPF group exhibited ileal epithelial hemorrhage, villi rupture, and recessive aberration in terms of pathological outcomes. However, when treated with GSLS, there was a significant improvement observed in the intestinal damage, and the recovery of intestinal villi was also visible.

Once the GSLS was administered, there was a reduction observed in the DAO of intestinal tissues in a dose-dependent fashion. These outcomes showcased the protective mechanism of GSLS in the intestinal injury recovery process. When the ROS gets deposited during oxidative stress in the organisms, it

can directly open the gates for Cytc precursors and caspases from mitochondria to cytoplasm. Further, the mitochondria release the cytochrome C, which activates caspase-9, activated caspase-3, and other apoptotic factors. This chain process ultimately results in cell death in intestinal tissues. The Bcl-2 family proteins can potentially inhibit the release of Cytc and, accordingly, cell apoptosis. However, Bax triggers the release of Cytc and advances the cell apoptosis process[29]. As per the literature, oxidative stress boosts the Bax, which in turn releases the Cytc from mitochondria to cytoplasm and accordingly activates the pro-caspase-3 to caspase-3, thus promoting the apoptotic process[29].

Limitations

Our study primarily focused on *in vitro* evaluations of the cytotoxic potentials, anticancer effects, and anti-HCV activity of the synthesized nanoparticles. While these findings provide important preliminary data, further *in vivo* studies are necessary to validate and confirm the observed effects in more complex biological systems. The study evaluated the effects of a single dose concentration of the synthesized nanoparticles. However, it is important to acknowledge that different concentrations may yield varying results. Further investigations involving a broader range of concentrations would provide a more comprehensive understanding of the dose-response relationship and potential therapeutic efficacy. Although we observed promising effects of the synthesized nanoparticles, the underlying mechanisms by which they exert their cytotoxic, anticancer, and anti-HCV activities remain to be fully elucidated. Future studies should aim to explore the specific molecular pathways and cellular interactions involved to provide a more comprehensive understanding of the nanoparticle's mode of action.

Conclusions

In the current study, the ascorbic acid was utilized in the galactosylation of Chitosan as a green method, replacing the sodium borohydride. In two *Bosci* extracts (*Boscia angustifalia* and *Boscia senegalensis*), the Nanochitosan was loaded under varying concentrations. High stability was exhibited by the synthesized Chitosan NPs, whereas the *Boscia angustifalia* extract recorded 46.58% encapsulation, while in the case of *Boscia senegalensis* extract, it was 9.77%. As mentioned earlier, the zeta potential of both extracts with NPs was found to be good, inferring good stability. In acidic media, the *Boscia angustifalia* extract was released from the NPs up to 40%, while under normal pH conditions, it was 60%. The NPs of all the concentrations, were found to be non-cytotoxic and exhibited a medium-level anticancer effect. When the two newly developed composites were evaluated against HCV in an *in-vitro* system, the whole set of samples exhibited anti-HCV activity with increasing concentration. In comparison, *Boscia angustifalia* exhibited higher anti-HCV activity than *Boscia senegalensis*. So, it can be concluded that *Boscia angustifalia* is a promising candidate for anti-HCV drugs to be used in future *in-vivo* studies.

Conflict of Interest

The authors declare that they have no conflict of interests.

Data Availability

All the data shown in the manuscript further queries can be communicated through the corresponding author by email.

Funding

The authors are thankful to the Deanship of Scientific Research at Prince Sattam bin Abdulaziz University for funding this work under the General Research Funding program grant code number (IF2/PSAU/2022/03/22763).

Ethics Approval

Ethical approval (No. MACA/2020/08/113) was obtained from the College of Life Science, Maulana Azad College of Arts and Science, Aurangabad, India. College of Life Science, Maulana Azad College of Arts and Science, Aurangabad, India approved the publication of data generated from this study.

Authors' Contributions

AB, SA, NA, AH, AA, and MA - concepts, design, data analysis, statistical analysis, manuscript preparation, manuscript review, and guarantor. HA, FA, DF, NEA, GA, AB, and MA - definition of intellectual content, literature search, experimental studies, data acquisition, manuscript editing.

ORCID ID

Abdulkarim S.B. Inshaya: 0000-0001-7663-3443
Suad A. Alghamdi: 0000-0002-8325-5994
Nahed S. Alharthi: 0000-0001-5597-5882
Ahmed Hjazi: 0000-0002-1129-6930
Abdullah A. Alqasem: 0009-0000-6022-1751
Deema Fallatah: 0000-0002-6801-3104
Nasser Eissa Almoammar: 0009-0000-6022-1751
Hassan H. Almasoudi: 0000-0002-6722-6667
Ghfren S. Aloraini: 0000-0002-7743-0012
Fahad M. Aldakheel: 0000-0001-8047-8650
MS. Aloahd: 0000-0003-0144-7608

References

1) Alangari A, Alqahtani MS, Mateen A, Kalam MA, Alshememry A, Ali R, Kazi M, AlGhamdi KM, Syed R. Iron oxide nanoparticles: Preparation, characterization, and assessment of antimicrobial and anticancer activity. Adsor Sci Technol 2022; 2022: 1-9.
2) Lewinski N, Colvin V, Drezek R. Cytotoxicity of nanoparticles. Small 2008; 4: 26-49.
3) Oberdörster G, Oberdörster E, Oberdörster J. Nanotoxicology: an emerging discipline evolving from studies of ultrafine particles. Environ Health Perspect 2005; 113: 823-839.
4) Arora S, Rajwade JM, Paknikar KM. Nanotoxicology and in vitro studies: the need of the hour. Toxicol Appl Pharmacol 2012; 258: 151-165.
5) Naisbitt DJ, Olsson-Brown A, Gibson A, Meng X, Ogese MO, Tailor A, Thomson P. Immune dysregulation increases the incidence of delayed-type drug hypersensitivity reactions. Allergy 2020; 75: 781-797.
6) Sies H. Oxidative stress: a concept in redox biology and medicine. Redox Biol 2015; 4: 180-183.
7) Wang CH, Wu SB, Wu YT, Wei YH. Oxidative stress response elicited by mitochondrial dysfunction: implication in the pathophysiology of aging. Exp Biol Med 2013; 238: 450-460.
8) Prajapati P, Gohel D, Shinde A, Roy M, Singh K, Singh R. TRIM32 regulates mitochondrial mediated ROS levels and sensitizes the oxidative stress induced cell death. Cell Signal 2020; 76: 109777.
9) Scherz-Shouval R, Elazar Z. Regulation of autophagy by ROS: physiology and pathology. Trends Biochem Sci 2011; 36: 30-38.
10) Feng ZQ, Chu X, Huang NP, Wang T, Wang Y, Shi X, Ding Y, Gu ZZ. The effect of nanofibrous galactosylated chitosan scaffolds on the formation of rat primary hepatocyte aggregates and the maintenance of liver function. Biomaterials 2009; 30: 2753-2763.
11) Park IK, Yang J, Jeong HJ, Bom HS, Harada I, Akaike T, Kim SI, Cho CS. Galactosylated chitosan as a synthetic extracellular matrix for hepatocytes attachment. Biomaterials 2003; 24: 2331-2337.
12) Kim TH, Park IK, Nah JW, Choi YJ, Cho CS. Galactosylated chitosan/DNA nanoparticles prepared using water-soluble chitosan as a gene carrier. Biomaterials 2004; 25: 3783-3792.
13) Khodabakhshaghdam S, Khoshfetrat AB, Rahbarghazi R. Alginate-chitosan core-shell microcapsule cultures of hepatic cells in a small scale stirred bioreactor: impact of shear forces and microcapsule core composition. J Biol Eng 2021; 15: 1-2.
14) Ohkawa H, Ohishi N, Tgi K. Assay for lipid peroxides in animal tissues by thiobarbituric acid reaction. Ann Chem 1979; 95: 351-358.
15) Zvezdova D. Synthesis and characterization of chitosan from marine sources in Black Sea. Annual Proceedings," Angel Kanchev" University of Ruse 2010; 49: 65-69.
16) Choi EJ, Kwon HC, Ham J, Yang HO. 6-Hydroxymethyl-1-phenazine-carboxamide and 1, 6-phenazinedimethanol from a marine bacterium, BrevibacteriumBrevibacterium sp. KMD 003, associated with marine purple vase sponge. J Antibiot 2009; 62: 621-624.
17) Miller GL. Use of dinitrosalicylic acid reagent for determination of reducing sugar. Anal Chem 1959; 31: 426-428.
18) Othman R, Vladisavljević GT, Thomas NL, Nagy ZK. Fabrication of composite poly (d, l-lactide)/montmorillonite nanoparticles for controlled delivery of acetaminophen by solvent-displacement method using glass capillary microfluidics. Colloids Surf B Biointerfaces 2016; 141: 187-195.
19) Mangino MJ, Murphy MK, Glabar GG. Protective effects of glycine during hypothermic renal ischemic reperfusion injury. Am J Physiol 1991; 261: 841-848.
20) Habig WH, Pabst MJ, Jakoby WB. Glutathione S-transferases. The first enzymatic step in mercapturic acid formation. J Biol Chem 1974; 249: 7130-7139.
21) Aebi H. Catalase. In: Methods of enzymatic analysis (Eds.: H.U. Bergmeyer). Academic Press Inc., New York, 1972; 2: 673-684.
22) Misra HP, Fridovich I. The role of superoxide anion in the autoxidation of epinephrine and a simple assay for superoxide dismutase. J Biol Chem 1972; 247: 3170-3175.
23) Muslim SN, Ali AN, Jawad RS, AL_Kadmy IM, Dwaish AS, Hussein NH. Biosafety of Handling of some pathogenic bacteria. INJC 2016; 16: 1-2.
24) Divya PV, Viswanadham BV, Gourc JP. Evaluation of tensile strength-strain characteristics of fiber-reinforced soil through laboratory tests. J Mater Civil Eng 2014; 26: 14-23.
25) Bahadar H, Maqbool F, Niaz K, Abdollahi M. Toxicity of nanoparticles and an overview of current experimental models. Iran Biomed J 2016; 20: 1.
26) Sabnis S, Block LH. Chitosan as an enabling excipient for drug delivery systems: I. Molecular modifications. Intl J Biol Macromol 2000; 27: 181-186.
27) Beltrán-Ortiz C, Peralta T, Ramos V, Durán M, Behrens C, Maureira D, Guzmán MA, Bastias C, Ferrer P. Standardization of a colorimetric technique for determination of enzymatic activity of diamine oxidase (DAO) and its application in patients with clinical diagnosis of histamine intolerance. World Allergy Organ J 2020; 13: 100457.
28) Gómez-Crisóstomo NP, López-Marure R, Zapata E, Zazueta C, Martínez-Abundis E. Bax induces cytochrome c release by multiple mechanisms in mitochondria from MCF7 cells. J Bioenerg Biomembr 2013; 45: 441-448.
29) Jürgensmeier JM, Xie Z, Deveraux Q, Ellerby L, Bredesen D, Reed JC. Bax directly induces release of cytochrome c from isolated mitochondria. Proceed Nat Aca Sci 1998; 95: 4997-5002.